Journal of Magnetism and Magnetic Materials 443 (2017) 261–266

Contents lists available at ScienceDirect

Journal of Magnetism and Magnetic Materials

journal homepage: www.elsevier.com/locate/jmmm

Research articles

Dynamic magnetic characteristics and relaxation of $Fe_{73.5}Cu_1Nb_3Si_{15.5}B_7$ nanocrystalline alloy under operating temperature and magnetizing frequency

Aina He, Shiqiang Yue, Anding Wang *, Chuntao Chang *, Xinmin Wang

Key Laboratory of Magnetic Materials and Devices, Zhejiang Province Key Laboratory of Magnetic Materials and Application Technology, Ningbo Institute of Materials Technology and Engineering, Chinese Academy of Sciences, Ningbo, Zhejiang 315201, China

ARTICLE INFO

Article history:
Received 2 June 2017
Received in revised form 20 July 2017
Accepted 21 July 2017
Available online 22 July 2017

Keywords:
Nanocrystalline alloy
Dynamic magnetic characteristic
Core loss
Complex permeability
Magnetic relaxation

ABSTRACT

The alternation of dynamic magnetic characteristics with operating temperature and magnetizing frequency in annealed $Fe_{73.5}Cu_1Nb_3Si_{15.5}B_7$ nanocrystalline alloy core was systematically studied by AC *B-H* loop tracer and complex permeability approach. It is found that the operating temperature below 160 °C has little influence on core loss when the induction (B) is less than 1.1 T. As B becomes higher, core loss measured at higher temperature becomes larger. The B and remanence (B_r) at 80 A/m under power frequency both decline slightly as the temperature goes up. Furthermore, the real part of permeability (μ') increases at first and then decrease with the rise of temperature. The peaks of the imaginary part of permeability (μ'') shift to higher frequency side with decreasing μ' over operating temperature. In addition, the variations of permeability dispersion with the elevated in the operating temperature of the annealed nanocrystalline core are explained by fitting to Havriliak-Negami (H-N) model, revealing that temperature impact on the magnetic relaxation time.

1. Introduction

With the rapid development of technology and concerning on energy saving, modern electronic devices tend to be miniaturized, lightweight, and high energy efficient. Fe-based nanocrystalline alloys have excellent combination of soft magnetic properties such as higher permeability (μ), lower coercivity (H_c), lower core loss (P), and better high-frequency characteristics, compared to conventional soft magnetic materials [1–4]. Therefore, these alloys are attractive and increasingly used in magnetic electronic devices, such as common mode chokes, pulse transformers, high frequency power transformers and sensors [5–7]. Since these devices usually work on the AC magnetic field with a variety amplitude and magnetization frequency (f), it is essential to understand the dynamic magnetic response of nanocrystalline alloy to the AC field. One of the most widely used methods to obtain dynamic response, including magnetic domain movement and magnetic relaxation for nanocrystalline alloy driven by AC field is the application of the complex permeability approach [8,9]. On the other hand, these magnetic cores always work on the temperature with upper limit of higher than 100 °C due to the external heating sources and their own energy losses. The core designers need to choose optimum magnetic materials to ensure the magnetic function and safety, including consideration of AC field and operation temperature condition. Therefore, it is important for the magnetic designer to knowledge the dynamic magnetic performance of magnetic cores at elevated operating temperatures.

Great efforts have been devoted to exhibit the various factors which effect on dynamic magnetization of nanocrystalline alloys, e.g. the amplitude of AC field [8], the magnetizing frequency [10,11], the cooling rate [12], the slight surface oxidation [13], the transverse field-induction anisotropy [14], and the annealing temperature [15,16]. In addition, Several nanocrystalline alloys, eg. FeCoCuNiSiB alloy [17], Finemet-type nanocrystalline alloy [18], and FeSiBNbCu alloy [19], have been a subject of investigation of their magnetic properties varied with temperature. However, the influence mechanism of operating temperature on magnetic dynamic performance and dynamic magnetic relaxation for nanocrystalline alloy core is still unclear. Havriliak–Negami (H-N) relaxation model is an empirical modification of the Debye relaxation model, assuming the broadening and asymmetric distributions of relaxation time. Despite this model is widely used for investigation of different relaxations in glassy system [20], bulk Z-type cobalt hexaferrite [21], soft magnetic bulk cores [22], etc.

* Corresponding authors.
E-mail addresses: anding@nimte.ac.cn (A. Wang), ctchang@nimte.ac.cn (C. Chang).

http://dx.doi.org/10.1016/j.jmmm.2017.07.080
0304-8853/

Study of magnetic relaxation behavior for nanocrystalline ribbon-wound cores from this aspect is not thorough.

In this study, we intend to provide a comprehensive view of the frequency dependence of magnetic dynamic characteristics including magnetic induction (B), remanence (B_r), core loss (P) and complex permeability under the operating temperature in an annealed ribbon-wound core based on an $Fe_{73.5}Cu_1Nb_3Si_{15.5}B_7$ nanocrystalline alloy. We have improved the magnetic properties on this alloy by utilizing two-step heat treatment process and controlled the formation of Cu clusters to further optimize the nanocrystalline structure [23]. Here, based on the optimum magnetic properties of this alloy at room temperature obtained in our previous work. The relations among the magnetic dynamic properties, magnetization frequency and operating temperature on the nanocrystalline alloy core are illustrated. Furthermore, the magnetic relaxation behavior is explored by using a Havriliak-Negami (H-N) model.

2. Experimental procedure

The experimental results were performed on toroidally wound cores of nanocrystalline alloy with nominal composition $Fe_{73.5}Cu_1Nb_3Si_{15.5}B_7$ (at.%). The precursor of nanocrystalline alloy was amorphous ribbon obtained by rapid quenching at a cooling rate of one million °C/s. The as-quenched ribbon with 21 μm thick, was cut into 15 mm wide, and then was wound automatically into the toroidal core with an inner diameter and outer diameter of 20 and 31 mm, respectively. Before measuring the dynamic magnetic characteristics, these core samples were subjected to two-step annealing progress to achieve uniform nanocrystalline structure and optimum magnetic properties at room temperature. During this heat treatment, the cores were isothermally pretreated at 400 °C for 1 h and then nanocrystallized at 560 °C for 1 h without applying an external magnetic field. A holder was used to protect the annealed toroidal core sample from vibration and from wire windings tightening. Coated copper wire which can bear the measurement temperature was chosen for the winding coil. The variation of dynamic magnetic properties with temperature were measured from room temperature (20 °C) to 160 °C regulated by putting the core in a muffle furnace.

In situ measurement for the operating temperature dependence of dynamic hysteresis loops and core loss in the nanocrystalline wound core were carried out by using AC B-H loop tracer under the different frequency of 50 Hz, 400 Hz and 1 kHz. The coated copper wire was 20 turns for the primary coil and provided with windings of 2 turns for the secondary coil, respectively.

Complex permeability, $\mu = \mu' - i\,\mu''$, at a frequency range from 50 Hz to 10 MHz and under elevated operating temperature of the nanocrystalline core with 20 turns of insulated copper wire in situ measured by means of an impedance analyzer (Agilent 4294) equipped with a test fixture (16047E). The amplitude of applied AC magnetic field was kept at very small value of about 0.1 A/m to ensure the regime of initial permeability. The measured frequency was swept with 501 discrete frequencies.

The complex permeability as a function of angular frequency is predicted by the Havriliak-Negami (H-N) relaxation model [22,24,25]. The H-N model is expressed as the following relations:

$$\hat{\mu}(\omega) = \mu_\infty + \frac{\mu_s - \mu_\infty}{\left[1 + (i\omega\tau_r)^{1-\alpha}\right]^\beta} \tag{1}$$

In this expression, $\hat{\mu}(\omega) = \mu'(\omega) - i\mu''(\omega)$ is the complex permeability, $\omega = 2\pi f$ is the angular frequency, i is the unit imaginary number, μ_∞ is the permeability at high frequency limit, μ_s is the static or low frequency permeability, and τ_r is the relaxation time, α is related to the width of the loss peak, β controls the asymmetry of the loss peak. The exponents α and β can take on values between 0 and 1.

The real part (μ') and imaginary part (μ'') of the complex permeability can be calculated as:

$$\mu'(\omega) = \mu'_\infty + (\mu'_s - \mu'_\infty)(1 + 2(\omega\tau_r)^{1-\alpha} + (\omega\tau_r)^{2(1-\alpha)})^{-\beta/2} \times \cos(\beta\phi) \tag{2}$$

$$\mu''(\omega) = (\mu''_s - \mu''_\infty)(1 + 2(\omega\tau_r)^{1-\alpha} + (\omega\tau_r)^{2(1-\alpha)})^{-\beta/2}\cos(\beta\phi) \tag{3}$$

with

$$\phi = \arctan\left(\frac{(\omega\tau_r)^{1-\alpha}\sin(\pi(1-\alpha)/2)}{1 + (\omega\tau_r)^{1-\alpha}\cos(\pi(1-\alpha)/2)}\right) \tag{4}$$

H-N model has been widely used to characterize the dynamic mechanical behaviors of polymers, transition metal and other materials. This study intends to investigate the dynamic magnetization processes of annealed $Fe_{73.5}Cu_1Nb_3Si_{15.5}B_7$ nanocrystalline alloy by using H-N model.

3. Results and discussion

The magnetic hysteresis loop is one of the most useful sources of information on magnetic properties from the application point of view. Fig. 1(a) shows the dynamic hysteresis loops of the annealed $Fe_{73.5}Cu_1Nb_3Si_{15.5}B_7$ nanocrystalline alloy ribbon-wound core at a frequency of 50 Hz were measured under operating temperature range from room temperature to 160 °C. As reported, the curie temperature of this alloy is 570 °C, which is significantly higher than the operating temperature. It can be observed from the AC hysteresis loops that the applied field (H) increases with increasing operating temperature when the magnetic induction (B) achieve same values, and the magnetic induction at 80 A/m decreases with increasing temperature. The temperature dependence of magnetic induction (B_{80}) and remanence (B_r) at the applied magnetic field of 80 A/m and a frequency of 50 Hz are presented in Fig. 1(b). It can be observed that the B_{80} and B_r both decline as the operating temperature goes up. The B_{80} decreases 1.2% at 50 °C, 4.3% at 70 °C, 5.3% at 100 °C, 7.1% at 130 °C, and 10% at 160 °C compared with that at room temperature, respectively. In many electronic application, nanocrystalline alloy cores are not operated near the saturation in order to keep the low core

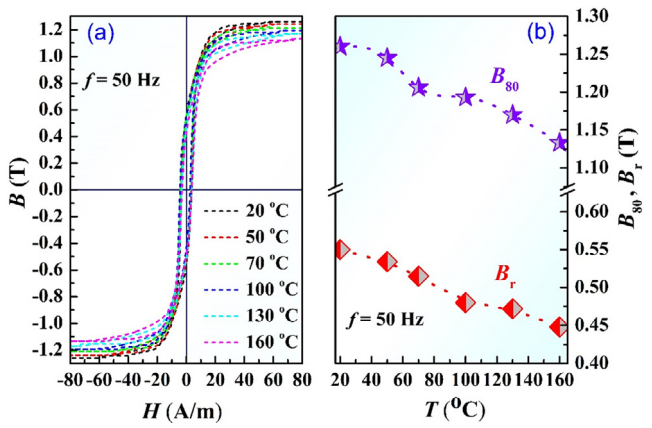

Fig. 1. Dynamic hysteresis loop (a), magnetic induction B_{80} and remanence B_r (b) for annealed $Fe_{73.5}Cu_1Nb_3Si_{15.5}B_7$ nanocrystalline alloy core measured at various temperature and at a frequency of $f = 50$ Hz. The inset illustrates the variation of B as a function of applied field H from 70 A/m to 80 A/m. Here, B_{80} is magnetic induction under the applied magnetic field of 80 A/m.

loss. The magnetic designers need to set suitable magnetic induction to meet the tolerable core losses and enough small core. It indicates that the application magnetic induction should be lower with operating temperature rises.

Owing to core loss is another critical parameter for designers, the temperature dependence of core loss at different frequency as a function of magnetic induction are also measured. As shown in Fig. 2(a), the effect of operating temperature on core loss is not obvious when the induction (B) is less than 1.1 T. As B becomes higher, core loss measured at higher temperature becomes larger. The temperature dependence of core loss for annealed $Fe_{73.5}Cu_1Nb_3Si_{15.5}B_7$ nanocrystalline alloy toroidal core at frequency of 400 Hz and 1 kHz under the induction of 1.1 T is illustrated in Fig. 2(b). Measured under the same temperature, the core loss shows a progressive increasing as the ascending frequency. The increment of core loss with frequency is due to the change of the effective field in the nanocrystalline core caused by generating an eddy current reaction field [26].It is interesting that at the frequency of 400 Hz and 1 kHz, the variations of core loss with operating temperature both reveal similar trends toward reduce at first and then rise at a frequency of 50 Hz.

Table 1 also shows the temperature dependence of coercivity (H_c) at 400 Hz and core loss (P) at 50 Hz for the annealed $Fe_{73.5}Cu_1Nb_3Si_{15.5}B_7$ nanocrystalline alloy. It is observed that the H_c at 1 T and P at 1.1 T both decline slightly at first and consequently increase as the temperature goes up. For example, The $H_{c1/400}$ and $P_{1.1/50}$ both reduce 1.5% and 2.3% at 50 °C compared with room temperature, respectively. On the other hand, the $H_{c1/400}$ and $P_{1.1/50}$ both increase 5.9% and 9.8% at 160 °C compared with room temperature.

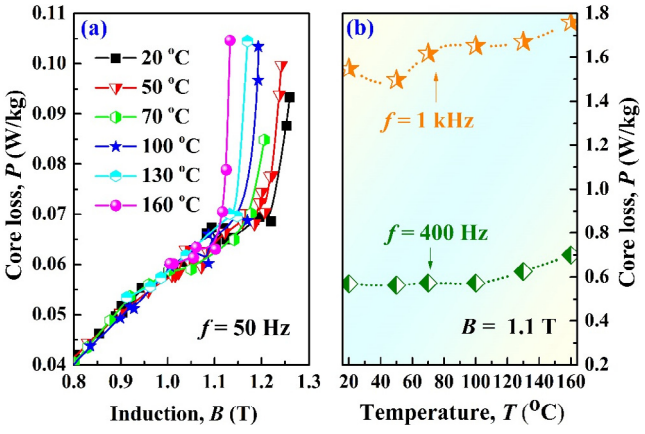

Fig. 2. Temperature dependence of core loss (a) at a frequency of f = 50 Hz as a function of magnetic induction intensity and (b) at frequency of 400 Hz and 1 kHz under the induction of 1.1 T for annealed $Fe_{73.5}Cu_1Nb_3Si_{15.5}B_7$ nanocrystalline alloy toroidal core.

In order to evaluate the thermal evolution of complex permeability for the annealed $Fe_{73.5}Cu_1Nb_3Si_{15.5}B_7$ nanocrystalline alloy ribbon-wound core, the real part μ' and imaginary part μ'' of complex permeability spectrums have been measured at the frequency range from 50 Hz to 10 MHz and temperature interval from room temperature to 160 °C. Fig. 3a depicts the frequency dependence of real permeability, μ' for the $Fe_{73.5}Cu_1Nb_3Si_{15.5}B_7$ alloy core at selected operating temperatures. Take into account the μ' measured under an applied magnetic field with a low amplitude, H_m = 0.1 A/m, we can regard these μ' as the initial real permeability. As the frequency goes up, the μ' measured at all operating temperatures exhibits similar dispersive behavior, where the values keep high and nearly constant in a wide frequency range from 50 Hz to 20 kHz at first, and subsequently decline to small values.

Fig. 3b displays the temperature variation of imaginary permeability, μ'' for the $Fe_{73.5}Cu_1Nb_3Si_{15.5}B_7$ alloy core at operating temperatures up to 160 °C. Unlike real permeability, the μ'' measured at all selected temperature exhibit low values in a wide frequency range from 50 Hz to 1 kHz, but they then grow up with further increasing frequency and show peaks for various temperatures at particular frequencies. The single peak of μ'' at a particular frequency, can be identified as relaxation frequency, f_r. In fact, beyond this relaxation frequency, the value of μ'' falls rapidly.

For the annealed $Fe_{73.5}Cu_1Nb_3Si_{15.5}B_7$ nanocrystalline alloy ribbon-wound core, these changes of the real part μ' and imaginary part μ'' of complex permeability with frequency under all selected temperatures can be interpreted in terms of the dynamic magnetization process and magnetic relaxation [27,28]. At low frequencies, domain walls are pinned, and these pinning sites are most probably on the surface of the nanocrystalline alloy ribbon. On the other hand, the dominant magnetization process is that domain walls are bulging and these motions are reversible. Thus, the μ' and μ'' are almost constant at low frequencies. Since eddy current loss increases and magnetic relaxation appears with increasing frequency. Therefore, as frequency goes up, the μ' decreasing toward very small values and the μ'' rising toward peak can be ascribed to the eddy current damping and magnetic relaxation dispersion. When the frequency goes up to f_r, the domain walls bulging can no longer follow the external applied field, the μ' drops and μ'' elevates on account of the relaxation dispersion.

Inset of Fig. 3a illustrates the relative change in real permeability normalize to its room temperature value versus operating temperature at different frequencies. For all three AC frequencies, the relative rates of change in μ' are positive and negative when the temperature below and beyond 130 °C, respectively. The highest positive relative rate of change in real permeability, about 15.9% under 50 Hz, 6.4% under 1 kHz, and 3.4% under 10 kHz, are both observed at 50 °C, respectively. The negative relative rate of change in real permeability, about 12.1% for 50 Hz, 10.4% for 1 kHz and −9.7% for 10 kHz, are all located at 160 °C, respectively. Further, it is noticed from Fig. 3 that the peaks of μ'' shift to higher frequency side with decreasing μ' over operating temperature, which accord with Snoek's relation [29].

Table 1
Dynamic magnetic properties of annealed $Fe_{73.5}Cu_1Nb_3Si_{15.5}B_7$ nanocrystalline alloy toroidal core measured under different operating temperatures.

Operating Temperature T (°C)	$B_{80/50}$ (T)	$B_{r80/50}$ (T)	$H_{c1/400}$ (A/m)	$P_{1.1/50}$ (W/kg)
20	1.26	0.55	3.37	0.064
50	1.25	0.53	3.32	0.063
70	1.21	0.52	3.43	0.065
100	1.19	0.48	3.45	0.067
130	1.17	0.47	3.51	0.070
160	1.13	0.45	3.57	0.071

Here, $B_{80/50}$ is magnetic induction intensity at 50 Hz under the applied magnetic field of 80 A/m, $B_{r80/50}$ is remanence at 50 Hz under the applied magnetic field of 80 A/m, $H_{c1/50}$ is coercivity at 400 Hz under the induction of 1 T, and $P_{1.1/50}$ is core loss at 50 Hz under the induction of 1.1 T.

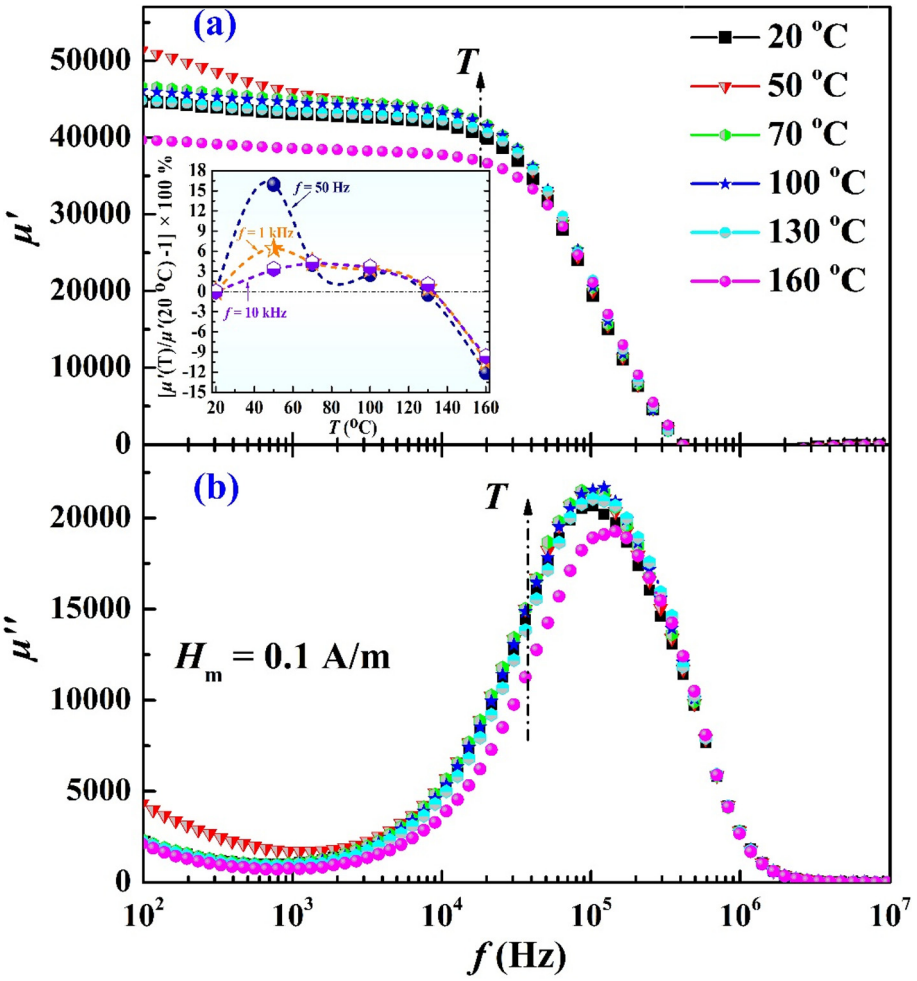

Fig. 3. The real part (μ', a) and the imaginary part (μ'', b) of the complex permeability as a function of frequency for the annealed $Fe_{73.5}Cu_1Nb_3Si_{15.5}B_7$ nanocrystalline alloy ribbon-wound core at selected operating temperatures and the constant magnetic field amplitude H_m = 0.1 A/m. The inset illustrates the relative change in real permeability normalize to its room temperature value vs. operating temperature at frequency of 50 Hz, 1 kHz, and 10 kHz.

Fig. 4 shows the Cole-Cole plots of the complex permeability of nanocrystalline $Fe_{73.5}Cu_1Nb_3Si_{15.5}B_7$ alloy core under various operating temperature. The alternation of μ'' with μ' has been depicted at different temperatures and under the magnetic field amplitude H_m=0.1 A/m. The corresponding frequency for each point increases from right to left. It can be observed from Fig. 4 that the shape of Cole-Cole plots is temperature dependent and semicircle. The smallest curvature is observed at the temperature of 160 °C. All these semicircles merge and terminate on the μ' axis at higher frequency side. There is no second semicircle observed indicating there is only nanocrystalline alloy core resistance exist. In addition, the domain wall movement displays a clear relaxation behavior, as affirmed by the semicircles in the Cole-Cole plots. The radius of semicircles variation with the growth of temperate indicates the change in relaxation time [30].

To further analyze the temperature dependence of dynamic magnetic processes for the annealed $Fe_{73.5}Cu_1Nb_3Si_{15.5}B_7$ nanocrystalline alloy, the experimental complex permeability is theoretical fitted by using the H-N model expressed by Eqs. (2) and (3). In the nonlinear curve fitting procedure, we consider the values of μ_s' and μ_s'' as the experimental real part and imaginary part of complex permeability measured at a low frequency of 50 Hz, respectively. Since there are no more active magnetization processes exist at high frequency limit, the value of μ_∞' and μ_∞'' are both equal to one [22]. Fig. 5 exhibits the experimental real part (μ') and imaginary part (μ'') of complex permeability spectra for annealed $Fe_{73.5}Cu_1Nb_3Si_{15.5}B_7$ nanocrystalline alloy toroidal core at selected operating temperature. The solid and dash lines are the nonlinear curve fits to real part and imaginary part of com-

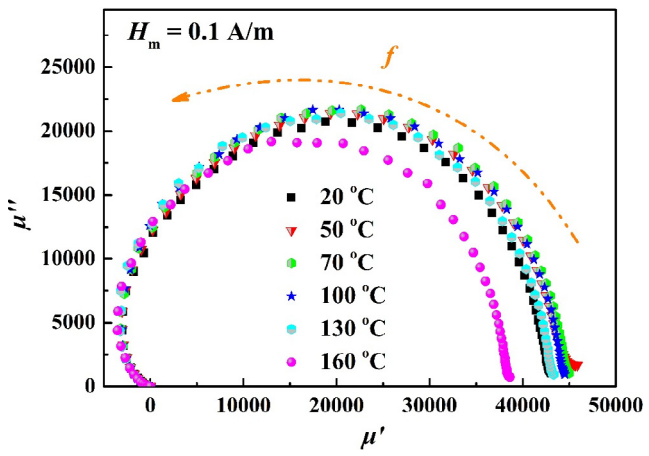

Fig. 4. Evolution of Cole-Cole Plots of the complex permeability for the annealed $Fe_{73.5}Cu_1Nb_3Si_{15.5}B_7$ nanocrystalline alloy toroidal core under selected operating temperatures and the magnetic field amplitude H_m = 0.1 A/m.

plex permeability measured at different temperature by using H-N model, respectively. It can be seen from Fig. 5 that the theoretical fitting curves well coordinate with the experimental real part and imaginary part of complex permeability curves. The goodness of fits for annealed nanocrystalline alloy at all measured operating temperatures is 0.998.

H-N model is able to describe relaxation behavior of metals or alloys. In this fitting, the exponents α, β, and relaxation time τ_r are related to the distribution of relaxation behavior and basically give an estimate of the dynamics of the magnetic relaxation process occurring in the sample. The α, β, and τ_r for the nanocrystalline alloy core versus temperature are obtained by the best fitting to experiment complex permeability using H-N model formulas. The results are depicted in Fig. 6. The values of α are 0.0078, 0.0175, 0.0044, 0.00189, 0.00082 and 0.000427 from room temperature to 160 °C. Accordingly, the values of τ_r are 1.85 μs, 1.91 μs, 1.86 μs, 1.80 μs, 1.69 μs and 1.45 μs from room temperature to 160 °C. As temperature goes up, α and τ_r both exhibit increase at first and then decrease, while β keeps nearly constant. The highest values of α and τ_r are both gained at 50 °C. These results indicate that the increment of investigated operating temperature cause the variation in the width of loss peak and relaxation time, which can explain the change of real part and imaginary part of complex permeability with increasing temperature.

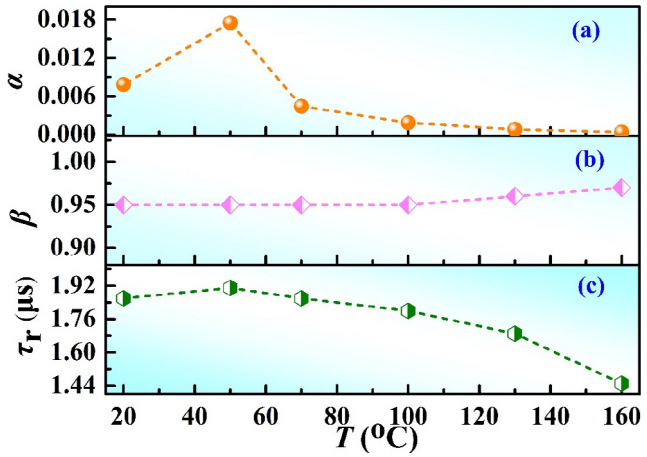

Fig. 6. Temperature dependence of and exponents α (a), β (b), and relaxation time τ_r (c) of H-N model obtained from the best fitting of experimental complex permeability spectra for annealed $Fe_{73.5}Cu_1Nb_3Si_{15.5}B_7$ nanocrystalline alloy core.

4. Conclusions

The operating temperature and frequency dependence of dynamic magnetic characteristics including magnetic induction, remanence, core loss and complex permeability of the annealed ribbon-wound core based on an $Fe_{73.5}Cu_1Nb_3Si_{15.5}B_7$ nanocrystalline alloy core were systematically investigated. It has been found that the induction B and remanence B_r at 80 A/m both decline as the operating temperature goes up. The effect of operating temperature on core loss is not obvious when the B is less than 1.1 T. As B becomes higher, core loss measured at higher temperature becomes larger. The H_c at 1 T and P at 1.1 T both decline slightly at first and consequently increase as the temperature goes up.

The complex permeability analysis reveals that high μ' and low μ'' values are obtained at low frequencies. The μ' rise up at first and then go down with the elevation in temperature. The peaks of μ'' shift to higher frequency side with decreasing μ' over operating temperature. Further, the variation of complex permeability with temperature of the nanocrystalline can be explained by H-N model. The relaxation time extracted from best fitting to H-N equations is found to increase firstly and then decrease with increasing operating temperature.

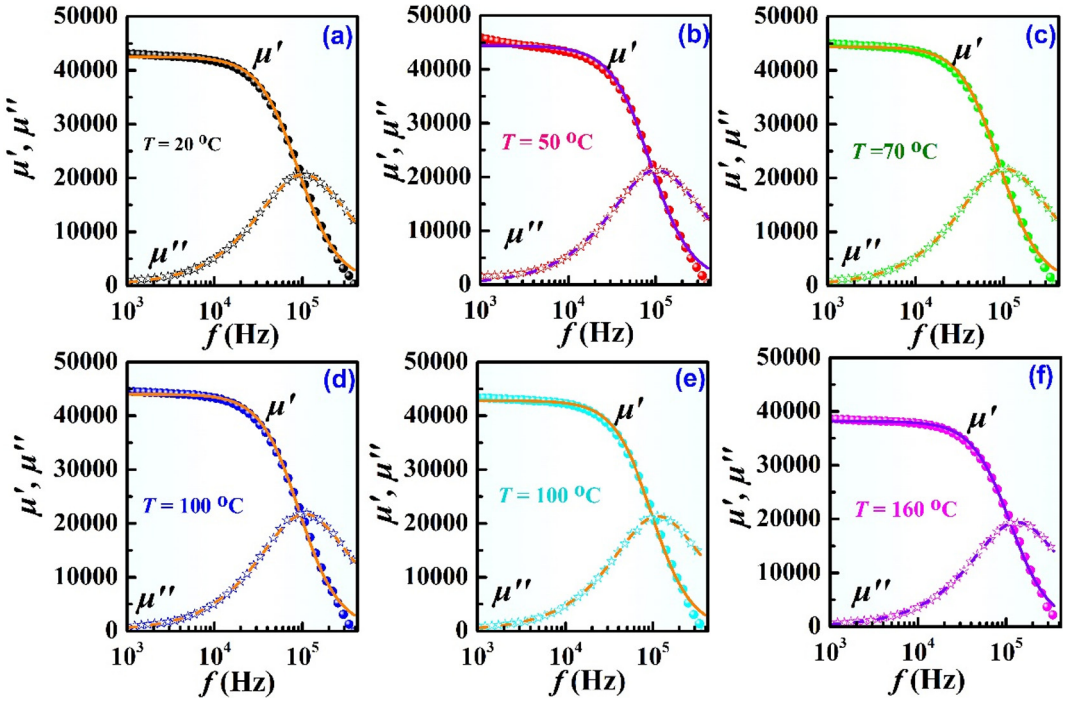

Fig. 5. Experimental real part (μ', ●) and imaginary part (μ'', ☆) of complex permeability spectra for annealed $Fe_{73.5}Cu_1Nb_3Si_{15.5}B_7$ nanocrystalline alloy toroidal core at selected operating temperature. The solid and dash lines are the nonlinear curve fits to real part and imaginary part of complex permeability measured at different temperature by using H-N model, respectively.

Acknowledgements

This work was supported by the National Natural Science Foundation of China (Grant No. 51601206, 51671206), and The National Key Research and Development Program of China (2016YFB0300501).

References

[1] M. Yousefi, K. Rahmani, M.S. Amiri, Kerahroodi, Comparison of microstructure and magnetic properties of 3% Si-steel, amorphous and nanostructure Finemet, J. Magn. Magn. Mater. 420 (2016) 204–209.
[2] G. Herzer, Modern soft magnets: Amorphous and nanocrystalline materials, Acta Mater. 61 (2013) 718–734.
[3] R. Hasegawa, Advances in amorphous and nanocrystalline materials, J. Magn. Magn. Mater. 324 (2012) 3555–3557.
[4] Y. Yoshizawa, S. Oguma, K. Yamauchi, New Fe-based soft magnetic alloys composed of ultrafine grain structure, J. Appl. Phys. 64 (1988) 6044.
[5] K. Takenaka, N. Nishiyama, A.D. Setyawan, P. Sharma, A. Makino, Performance of a prototype power transformer constructed by nanocrystalline Fe-Co-Si-B-P-Cu soft magnetic alloys, J. Appl. Phys. 117 (2015) 17D519.
[6] M.A. Willard, M. Daniil, Chapter four – nanocrystalline soft magnetic alloys two decades of progress, in: K.H.J. Buschow (Ed.), Handbook of Magnetic Materials, Elsevier, 2013, pp. 173–342.
[7] J. Petzold, Applications of nanocrystalline softmagnetic materials for modern electronic devices, Scr. Mater. 48 (2003) 895–901.
[8] X. Mao, Z. Ke, W. Zou, Q. Lin, Z. Qin, Y. Wu, Effect of thermal treatment on the magnetization processes of nanocrystalline Fe80Ge3Nb10B7 alloys, J. Magn. Magn. Mater. 324 (2012) 389–393.
[9] J. Füzer, S. Dobák, P. Kollár, Magnetization dynamics of FeCuNbSiB soft magnetic ribbons and derived powder cores, J. Alloy. Compd. 628 (2015) 335–342.
[10] S. Chakraborty, K. Mandal, D. Sakar, V.J. Cremaschi, J.M. Silveyra, Dynamic coercivity of Mo-doped FINEMETs, Physica B 406 (2011) 1915–1918.
[11] N. Derebasi, R. Rygal, A.J. Moses, D. Fox, Variation of magnetic properties of toroidal cores with magnetizing frequency, J. Magn. Magn. Mater. 215 (2000) 611–613.
[12] W. Qin, K. Pen, W.L. Gao, F. Xu, G. Ni, Y.W. Du, Effect of cooling rate on dynamic magnetization of Fe86Zr7B6Cu nanocrystalline alloy, Mater Res Bull 37 (2002) 1393–1399.
[13] F. Xu, W. Qin, K. Peng, W. Gao, Y. Du, Effect of slight surface oxidation on the dynamic magnetization of nanocrystalline FeNbBCu ribbons, Mater. Lett. 57 (2003) 4227–4231.
[14] S. Flohrer, R. Schäfer, J. McCord, S. Roth, L. Schultz, F. Fiorillo, W. Günther, G. Herzer, Dynamic magnetization process of nanocrystalline tape wound cores with transverse field-induced anisotropy, Acta Mater. 54 (2006) 4693–4698.
[15] Y. Ding, S. Zhao, X. Liu, Y. Long, R. Ye, Y. Chang, F. Wan, The influence of annealing temperature on AC magnetic properties of Fe–Co–Cu–Nb–Si–B nanocrystalline alloy, Mater. Lett. 62 (2008) 1376–1378.
[16] H. Liu, C. Yin, X. Miao, Z. Han, D. Wang, Y. Du, Permeability spectra study of Fe73.5Si13.5B9Cu1Nb3−xAlx (x = 0, 0.1, 0.2, 0.4, 0.8 and 1.6), J. Alloy. Compd. 466 (2008) 246–249.
[17] R. Kolano, A. Kolano-Burian, J. Szynowski, L. Varga, F. Mazaleyrat, T. Kulik, N. Wojcik, L. Winczura, L. Kubica, Dependence of magnetic properties of the Fe-Co-Cu-Nb-Si-B nanocrystalline alloys on magnetic field frequency and temperature, Mater. Sci. Eng. A-Struct. Mater. Prop. Microstruct. Process. 375 (2004) 1072–1077.
[18] M. LoBue, V. Basso, P. Tiberto, C. Beatrice, G. Bertotti, Magnetization process and magnetic viscosity in soft nanocrystalline materials at elevated temperature, J. Magn. Magn. Mater. 226-230, Part 2, (2001) 1487–1489.
[19] A. Lekdim, L. Morel, M.-A. Raulet, Magnetic ageing study of high and medium permeability nanocrystalline FeSiCuNbB alloys, J. Magn. Magn. Mater. 428 (2017) 260–268.
[20] R. Hilfer, H-function representations for stretched exponential relaxation and non-Debye susceptibilities in glassy systems, Phys Rev E 65 (2002) 061510.
[21] F.R. Daró, A.C.C. Migliano, G.P. Zanella, A.K. Hirata, Y.C. De Polli, M.C.B. Salvadori, The effect of magnetic domain walls on the complex permeability of bulk Z-type cobalt hexaferrite along both W and Y-phases, Mater. Chem. Phys. 170 (2016) 12–23.
[22] S. Dobák, J. Füzer, P. Kollár, M. Strečková, R. Bureš, M. Fáberová, A comprehensive complex permeability approach to soft magnetic bulk cores from pure or resin coated Fe and pulverized alloys at elevated temperatures, J. Alloy. Compd. 695 (2017) 1998–2007.
[23] Y. Han, A. Wang, A. He, C. Chang, F. Li, X. Wang, Improvement of magnetic properties, microstructure and magnetic structure of Fe73.5Cu1Nb3Si15.5B7 nanocrystalline alloys by two-step annealing process, J. Mater. Sci.: Mater. Electron. 27 (2015) 3736–3741.
[24] S. Havriliak, S. Negami, A complex plane representation of dielectric and mechanical relaxation processes in some polymers, Polymer 8 (1967) 161–210.
[25] S. Havriliak, S. Negami, A complex plane analysis of α-dispersions in some polymer systems, J. Polym. Sci. Part C: Polym. Symposia 14 (1966) 99–117.
[26] J. Szczyglowski, Influence of eddy currents on magnetic hysteresis loops in soft magnetic materials, J. Magn. Magn. Mater. 223 (2001) 97–102.
[27] I. Betancourt, Magnetization dynamics of amorphous ribbons and wires studied by inductance spectroscopy, Materials 4 (2011) 37–54.
[28] R. Valenzuela, Low-frequency magnetoimpedance:domain wall magnetization processes, Phys. B 299 (2001) 280–285.
[29] A. Jawad, S.S.Z. Ashraf, Complex permeability and optical studies of Cr + 3 doped nano-structured γ-Fe2O3 synthesized by auto-combustion technique, J. Alloy. Compd. 569 (2013) 13–21.
[30] A. He, A. Wang, S. Yue, C. Zhao, C. Chang, H. Men, X. Wang, R.-W. Li, Dynamic magnetic characteristics of Fe78Si13B9 amorphous alloy subjected to operating temperature, J. Magn. Magn. Mater. 408 (2016) 159–163.